

# RSC Advances

This article can be cited before page numbers have been issued, to do this please use: Y. Shen, L. Lin, H. Qiu, W. Zou, Y. Qian and H. Zhu, *RSC Adv.*, 2015, DOI: 10.1039/C4RA12108B.



This is an *Accepted Manuscript*, which has been through the Royal Society of Chemistry peer review process and has been accepted for publication.

*Accepted Manuscripts* are published online shortly after acceptance, before technical editing, formatting and proof reading. Using this free service, authors can make their results available to the community, in citable form, before we publish the edited article. This *Accepted Manuscript* will be replaced by the edited, formatted and paginated article as soon as this is available.

You can find more information about *Accepted Manuscripts* in the [Information for Authors](#).

Please note that technical editing may introduce minor changes to the text and/or graphics, which may alter content. The journal's standard [Terms & Conditions](#) and the [Ethical guidelines](#) still apply. In no event shall the Royal Society of Chemistry be held responsible for any errors or omissions in this *Accepted Manuscript* or any consequences arising from the use of any information it contains.

**The Design, Synthesis, *in vitro* Biological Evaluation and Molecular Modeling of Novel Benzenesulfonate Derivatives Bearing Chalcone Moieties as Potent Anti-microtubulin Polymerization Agents**

**Yu-Ning Shen<sup>†</sup>, Lin Lin<sup>†</sup>, Han-Yue Qiu<sup>†</sup>, Wen-Yan Zou, Yong Qian\*, Hai-Liang Zhu\***

*State Key Laboratory of Pharmaceutical Biotechnology, Nanjing University, Nanjing 210093, China.*

\*Corresponding author. Tel. & fax: +86-25-83592672; e-mail: [zhuhl@nju.edu.cn](mailto:zhuhl@nju.edu.cn)  
(H.-L. Zhu),\_

<sup>†</sup> These authors contributed equally to this work.

## Abstract

A series of novel 3,4,-dimethoxybenzenesulfonate derivatives containing a chalcone-structure were synthesized and evaluated for their anti-proliferative activity against HepG2, HCT-116, MCF-7 and Hela cell lines, as well as the effects of compound **10b** on mitotic arrest and cell cycle of MCF-7 carcinoma cell line. Most importantly, the results of DAPI staining under co-focal microscope justified that compound **10b** functioned even at relatively low concentration. The analogues showed a potent bio-activity towards tumor cells with  $IC_{50}$  values at nano-mole class, compared with those of positive control drug *Colchicine*, whose  $IC_{50}$  were 150.4 nM for MCF-7, 123.9 nM for HepG2, 125.4 nM for HCT-116 and 131.4 nM for Hela cells. Also, a molecular docking modeling was utilized to reveal the binding mode of derivatives and microtubule. Among all the synthesized compounds, compound **10b** stands out as  $IC_{50}$  values against all the selected cell lines were at average 80 nM (in which the values against MCF-7 and HepG2 were similar; about 79.2 nM). In this research, we gave strong evidence upon the optimized stratagem for ligands targeting the colchicine-binding site on microtubules, explaining the attribution that the analogues were designed upon the structure of chalcone and *Combretastatin A-4*.

## Keywords

Microtubulin inhibitors

Combretastatin A-4

Benzenesulfonates

Docking

DAPI staining

## Introduction

A steadily increasing focus has been drawn to the treatment of cancers along with the development of human health care, in that cancers and tumors are one of the most intimidating threats to the public health. Tumor cells differentiate from normal cells enormously in the propagation rate, to inhibit the cell division, therefore, is one of the fundamental methods to treat cancers. In the process of cell division, microtubule plays an essential role; as well as in the process like maintenance of cell shape, regulation of motility, cell signaling, intracellular transport, and segregation of chromosomes<sup>1, 2</sup>, which hence makes it a significant target for the anti-tumor drug design. Some natural products, which are divided into two categories in general, are reported to demonstrate potent effects on interfering dynamics of microtubules: stabilizing agents versus destabilizing agents. Colchicine (Figure 1a) with its analogues, combretastatins, vinca alkaloids<sup>3</sup> function as destabilizing agents which inhibit microtubulin polymerization; taxanes, contrarily function as stabilizing microtubules by enhancing assembly. Since the past decades, some natural products were extracted and reported with the ability to combine to the colchicine-binding site on microtubules, among which is Combretastatin A-4(CA-4, Figure 1b) that derived from the South African tree *Combretum caffrum*. It demonstrated a potent antimitotic activity, also presented a vascular interruptive activity, and furthermore, the generally agreeable way that CA-4 causes mitosis arrest is effects on mitotic phases G2/M phase<sup>4, 5</sup>. The Structure-Activity Researches (SARs) of CA-4 had been focused on the modulations on A-ring, olfenic bridge and B-ring<sup>5-8</sup>, thereby a conclusion was drawn that it is remarkably useful to maintain the 3, 4, 5-trimethoxyl moiety in A-ring, a *cis*-alkenyl configuration in the bridge, and the hydroxyl group on B-ring so as to keep a relatively considerable activity. According to Stephen L<sup>9</sup>, etc., *cis*-alkene can be substituted by the sulfonates, also partially attributed to the cost of starting materials and the difficulty in the reactions, the A-ring with the bridge was modulated to 3,4-dimethoxyl bezensulfonate in our research.

On the other hand, according to past reports<sup>10, 11</sup>, chalcones demonstrated an anti-proliferative effect on cancer cells. Kerr D J<sup>12</sup> reported the chalcone analogues of

CA-4, which is a tough evidence of the chalcones' antitumor activities. Besides, lots of reports have proved that the chalcone analogues of CA-4 with potent biological activities<sup>10-13</sup>. Some work has been done by our group to optimize the CA-4 analogues and the methods of relevant biological assays and molecular imitations were still used in this research<sup>14, 15</sup>.

Hence, based on the Twin-drug Principle, we designed a series of benzenesulfonates derivatives **1b-19b** joint with chalcone parts so as to magnify the inhibitory activities towards the cancer cells. The structures of the compounds **1b-19b** (Table 1) were tested with imitative docking with the microtubule crystal (PDB code: 1SA0), with several compounds showing profoundly high absolute values of interaction energy. Our present research mainly focused on the derivatives' chemical and biological characteristics in regard of their basic structures as in the X-ray single crystal diffraction results; their inhibitory competency on several tumor cell lines evaluated from their IC<sub>50</sub> values, effects on the apoptosis and cell cycle. An immune-fluorescent staining assay virtually showed the ability on mitotic arrests on the human breast cancer cell, in the regard of morphological variations between the living carcinoma cells and mitotic ones of MCF-7 cell line.

## Results and Discussion

### 2.1 Chemistry

The synthetic route for the 3, 4,-dimethoxybenzenesulfonates derivatives **1b-19b** is outlined in Scheme 1. The intermediate chalcones (**1a-19a**) were prepared with the reported methodologies and protocol<sup>16</sup> as in the Claisen-Schmidt Condensation of substituted acetophenones with salicylaldehyde **1a-17a**, and substituted salicylaldehydes with acetophenone **18a, 19a** with the presence of hydroxide sodium aqueous solution; yielding rates were in a range of 70%-90%. Then the chalcones **1a-19a** were treated with 3,4,-dimethoxybenzenesulfonates under the sulfonation condition reported<sup>17</sup> to obtain the targeting products **1b-19b**, which were reported originally from our research. All the targeting products were purified with column chromatography before recrystallization in the 25 °C to 30 °C in ethanol/ ethyl acetate

solutions. All of the synthetic compounds gave satisfactory spectroscopic analysis, which were in full accordance with their assigned structures. Specifically, the X-ray crystallography of compound **10b** justified its structure (Figure 8, also see experimental parts 4.4).

## 2.2 Biological Evaluation

In the regard of anti-proliferative activities, the compounds were evaluated via MTT assay against MCF-7 (human breast carcinoma cell line), HepG2 (human liver carcinoma cell line), HCT116 (human colorectal carcinoma cell line), and Hela cells. Meanwhile the compounds were also evaluated toxicity towards normal cells 293T (human embryonic kidney cells) via MTT assay, whose materials and measurements are shown in experimental part 4.5. The results are summarized in Table 2, that the tested sulfonate derivatives exhibit appreciable anti-proliferative effects on the cell lines.  $IC_{50}$  values of these compounds against four carcinoma cell lines are distributed in a range of 70-190 nM; the inhibitory activities against the distinctive cells tended likewise.

Besides the anti-proliferative activities against carcinoma cells as described above, the compound **10b** was evaluated for its tubulin polymerization inhibitive activity versus positive control CA-4 (Table 3). The results showed that compound **10b** could bind to colchicine-binding site similarly as CA-4 did.

However, after a careful scrutiny towards the last row in Table 2, will it be not difficult to summarize that all the targeting products exhibited more potent toxic damages against 293T cell line, which made it a further focus to optimize this series upon lessening the toxicity and heightening the selectivity towards carcinoma cells.

Compared from the results shown in Table 2, the positive control colchicine effected on MCF-7 cell line with a very high activity ( $IC_{50} = 150.4$  nM) comparing to those of HepG2 ( $IC_{50} = 123.9$  nM), HCT-116 ( $IC_{50} = 125.4$  nM), and Hela cells ( $IC_{50} = 131.4$  nM), however, most compounds evaluated for the  $IC_{50}$  values manifested a relatively smaller value than that of colchicine's. Among them is the compound **10b**, which is one of the most potent agents against MCF-7 ( $IC_{50} = 79.2$  nM) and likewise

against other cell lines (79.2 nM, 81.34 nM, 86.8 nM, for HepG2, HCT-116, and Hela cells, respectively). Compound **10b** hence was selected to be evaluated the effects on apoptosis and mitotic arrests.

The structure-activity relationships (SARs) are depicted combining the data from Table 1 and Table 2. First, comparing the  $IC_{50}$  values of compound **17b**, **18b**, **19b** with those of **1b** to **16b**, substitutes on  $R_1$ - $R_6$  are better stratagems than substitutes on  $R_7$ - $R_9$ . Second, there is a general pattern for electron-donating groups and electron-withdrawing groups on  $R_1$ - $R_6$ . From each row,  $IC_{50}$  values of compound **2b** overweighed those of compound **4b**; methyl, methoxy, and ethoxy groups on *para*-, *meta*-, *ortho*- substitute, gave better inhibitory activity than nitro and halogen substituted compounds. Last, the compounds with substitution at the *para* were of better activity than those with substitution at the *ortho* and *meta* position. For example,  $IC_{50}$  value of **2b** (*para*-methoxy substituted) against MCF-7 cells (83.1 nM) is smaller than that of **12b** (*meta*-methoxy substituted, 107.4 nM). Similarly, compound **4b** (*para*-nitro substituted) has a better activity against MCF-7 cells ( $IC_{50}$  = 110.3 nM) than **9b** (*ortho*-nitro substituted,  $IC_{50}$  = 113.4 nM).

The death pattern of MCF-7 cells treated with compound **10b** (200 nM) was depicted in the Figure 2. The morphological changes between MCF-7 cells without or with the treatment of compound **10b** are manifest. DAPI can partially penetrate into the nucleus to stain nuclear DNA; thereby a relatively less intensive blue fluorescence will be captured if the nucleus is intact. While the apoptotic cells show intensive blue fluorescence of DAPI by staining of DAPI more, in that the permeability of nuclear membrane of apoptotic cells changes. Except for the increasing fluorescent intensity, the cytological morphology differs in apoptotic cells and normal cells. Compared to Figure 2a, the apoptotic cells in Figure 2b showed not only a much higher fluorescent intensity, but also the nucleus were irregularly edged with the chromatins unevenly stained. It is the typical characteristics of the apoptotic cells. Furthermore, a flow cytometry was used to further analyze the apoptosis. The MCF-7 cells were cross stained with Annexin V/PI<sup>18</sup>, and then the results were shown in Figure 3. Annexin V

binds with phosphatidylserine (PS) at the outer plasma membranes, which refined only to apoptotic cells. Therefore, the apoptotic cells are distinguished from intact ones, which are the (FITC labelled) annexin V-negative ones. Besides, the double labelling with propidium iodide (PI) can further quantitatively discriminates the damaged cells and necrotic ones. To conclude, the results from Figure 3 quantitatively shows intact cells (FITC-/PI-, Q4), apoptotic cells (FITC+/PI-, Q3), necrotic cells (FITC+/PI+, Q2), and damaged ones (FITC+/PI+, Q1). It is conspicuous that along the concentration of compound **10b** added up from 0 to 200 nM, the percentage of apoptotic cells and necrotic ones gave a relative increase as well. One thing should be noted that the necrotic cells added at the meantime, which mainly due to a long time treatment with compound **10b** as in the 24 hours incubation.

To determine the effects of the derivatives upon mitotic arrest and the effects on cell cycle concerning concentration, particularly, at nanomole level, a flow cytometry<sup>19</sup> was carried out, whose results were shown in Figure 4 and Figure 5. After 24 hours of treatment of compound **10b** as in the concentration order from 0 to 200 nM in the culture of MCF-7 cells, it can be evidenced that along with the concentration added yet still at a nanomole level, the percentage of cells arrested at the G2/M phases gave a positively related increase. Usually, the optimal ratio of CV of G2/M phase to G1 phase is expected less than 1<sup>19</sup>, which showed a consistence in Figure 4a, vehicle. When the concentration of compound **10b** added to 200 nM in Figure 4d, the ratio of DNA concentrations of GG2/M phase to G1 phase was nearly 2.

### 2.3 Molecular Docking

In the regard of the interaction of the derivatives and the microtubules, a Docking molecular modeling was used. Raimond B.G. Ravelli<sup>20</sup> gave a detailed description of microtubulin colchicine-binding site in 2004, which was justified by a crystal structure of DAMA-colchicine- microtubule complex (PDB code: 1SA0). The colchicine-binding site was mostly buried in the intermediate domain of  $\beta$  subunit, while surrounded by strands S8 and S9, loop T7 and helices H7 and H8. Buried-in

structure on the active site making it less likely for the compounds to fit deep in the domain, so a movement of T7 loop and H8 helix facilitates.

The results obtained from docking imitation were presented in Figure 6 and Figure 7. Researches have proved that methoxyl group on the A-ring on colchicine can be linked with cys241<sup>21</sup>. Our products, on the contrary, interacted with microtubules in a distinct way. The compound **6b** was fit in the colchicine-binding site with the lowest absolute value of interaction energy (Figure 6a, and Figure 6b). A strong pi-pi bond stabilizes the interaction between the LYS352 amino acid residue and the conjugated system, also a hydrogen bond happens accessorially between ASN101 and the methoxyl group. As the surface model of microtubule-ligand interaction in Figure 7, it reveals that the basic structure could be embedded into the active site, which makes it of more likelihood to be on-target. The binding mode of the analogues and the colchicine site predicted in the computational docking could be regarded as a consultation, we assumed that compound **10b** with the ethoxy group presented higher activity partially attributed to the stability of phenol ring on chalcone part that the ethoxy group helped with donating electrons, besides, ethoxy group inserted in the residue-slots near the active site.

#### 2.4 Western blot analysis

To test the ability of series to combine with colchicine-binding site, causing the mitotic arrest, a western blotting was conducted on MCF-7 cells after 10 hours treatment of compound **10b** (200 nM) and positive control Colchicine (200 nM). As were shown from Figure 9, after 10h treatment of colchicine and **10b**, histone remained similar amounts, P-histone, on the contrary, has given a rise. As was reported before<sup>22, 23</sup>, the phosphorylated histone is a significant marker of mitosis, the increases of P-histone, specifically the one treated with **10b**, has steadily proved that the compound **10b** had effects on mitosis, even in a more favorable way, as colchicine.

#### Conclusion

In this research, a series of benzenesulfonate derivatives have been synthesized and evaluated for their anti-proliferative activity ( $IC_{50}$  values) against MCF-7, HeLa, HCT-116, Hep G2 carcinoma cell lines, together with toxicity towards 293T cells as well. The derivatives exhibited potent inhibitory activity at a nanomolar level. Among the series, compound **10b** acted out ubiquitous strong effects on those four carcinoma cells (approximately 80 nM in a common place) and, a relatively low toxicity towards normal cells. Therefore, a flow cytometric research regarding the effects on apoptosis and cell cycle was committed upon compound **10b** at a soundly low concentration. With the auxiliary support from fluorescent PI staining assay, we justified how **10b** induced a mitotic arrest and apoptosis in the end. Then a molecular docking evidenced our prediction that the derivatives could interact with microtubules intimately; by the establishment of a pi-pi bond and two strong hydrogen bonds. Also, it was expected to fit in the embedded active site on the microtubules. The research somehow revealed the prospectively optimizational orientation for this series of compounds, which is also the future focus for this kind of designing upon the similar structure, namely, enhancement of the selectivity towards the mutant cells instead of making effects on both normal cells and carcinoma cells.

## Experimental Section

### 4.1 Materials and Methodologies

All of the synthesized compounds were assessed by thin layer chromatography (TLC), proton nuclear magnetic resonance ( $^1H$  NMR).  $^1H$  NMR spectra were measured on a Bruker AV-300, AV-400 or AV-500 spectrometer with tetramethylsilane (TMS) as an internal reference ( $\delta=0$ ) at 25 °C. Chemical shifts are reported in parts per million (ppm) using the residual solvent line as internal standard. Splitting patterns are designed as *s*, singlet; *d*, doublet; *t*, triplet; *m*, multiplet. Analytic thin-layer chromatography (TLC) was performed on the glass-backed silica gel sheets (silica gel 60 Å GF254). All compounds were detected using UV light (254 nm or 365 nm).

## 4.2 General protocols for synthesis of chalcones 1a-19a

Procedures for the synthesis of **1a-19a** (except for **3a**, **4a**, **9a**, **14a**):

Substituted acetophenones (5 mmol) and salicylaldehyde (5 mmol) were mixed in methanol (40 mL) in an ice bath. Then NaOH aqueous solution (40%, 10 mL) was added dropwise to the mixture maintaining in the ice bath. Then the stirring continued in the room temperature overnight. Then the mixture was washed by cold distilled water, neutralized with HCl solution (1 M), during which a precipitation appeared. After filtration, the residue was recrystallized in ethanol and estate ether at the room temperature then washed with water, to obtain the purified products.

Procedures for the synthesis of **3a**, **4a**, **9a** and **14a**:

To the mixture of substituted acetophenones (5 mmol) and salicylaldehyde (5 mmol) in methanol (40 mL), KOH (2 e.q., 10 mmol) was added and continuously stirred for 30min. Then the mixture was removed to room temperature, reflux at 80 °C for 24 hours. Then the mixture was washed and neutralized with HCl diluted solution (1 M), during which a precipitation appeared. After filtration, the residue was recrystallized in ethanol and acetate ether at the room temperature, and then washed with water to obtain the products.

## 4.3. General protocols for synthesis of benzenesulfonate derivatives 1b-19b

To the mixture of compound 3-(2-hydroxyphenyl)-1-*p*-tolylprop-2-en-1-one (**1a**) (2 mmol) and triethylamine (2 mL) in dichloromethane (20 mL) add 3,4-dimethoxybenzene-1-sulfonyl chloride (2 mmol) dropwise for over 20 min, stirring continuously in room temperature for two hours. The reaction mixture was washed with saluted brine and acetate ether (100 mL). The organic layer was dried with anhydrous sodium sulfate and the solvent was removed to obtain a rough solid product. The product then was purified with column chromatography, with developing solvents ethyl acetate (20 mL) in petroleum ether (400 mL). The purified product was obtained after the recrystallization in ethyl acetate and ethanol.

#### 4.3.1(*E*)-2-(3-Oxo-3-*p*-tolylprop-1-enyl)phenyl-3,4-dimethoxybenzenesulfonate

##### (1b)

m.p. 179-182 °C. <sup>1</sup>H NMR (400 MHz, CDCl<sub>3</sub>) δ: 7.48 (dd, *J* = 7.7, 1.2 Hz, 1H), 7.36 ~ 7.27 (m, 3H), 7.25 (d, *J* = 6.4 Hz, 1H), 7.17 (ddd, *J* = 18.5, 9.9, 5.1 Hz, 5H), 7.01 (d, *J* = 2.1 Hz, 1H), 6.84 (d, *J* = 16.1 Hz, 1H), 6.67 (d, *J* = 8.6 Hz, 1H), 3.69 (d, *J* = 11.9 Hz, 6H), 2.30 (s, 3H). <sup>13</sup>C NMR (101 MHz, CDCl<sub>3</sub>) δ: 188.45 (s), 163.29 (s), 153.37 (s), 151.80 (s), 141.22 (s), 137.53 (s), 128.15 (d, *J* = 9.6 Hz), 127.89 (s), 127.65 (d, *J* = 11.9 Hz), 127.35 (s), 125.44 (s), 124.99 (s), 123.76 (s), 120.45 (s), 118.97 (s), 113.39 (s), 113.17 (s), 110.98 (s), 110.51 (s), 56.69 (d, *J* = 11.3 Hz), 21.53 (s). IR (KBr, ν, cm<sup>-1</sup>): 3412, 3299, 3060, 2945, 1709, 1650, 1547, 1508, 1479, 1373, 1281, 1192, 1141, 1028, 968, 930, 897, 828, 749, 697, 495. MS (ESI) *m/z*: 438.1 (M<sup>+</sup>), calculated MS 438.49.

#### 4.3.2(*E*)-2-(3-(4-Methoxyphenyl)-3-oxoprop-1-enyl)phenyl-3,4-dimethoxybenzene sulfonate (2b)

m.p. 180-183 °C. <sup>1</sup>H NMR (300 MHz, CDCl<sub>3</sub>) δ 7.94 (d, *J* = 8.6 Hz, 2H), 7.64 ~ 7.52 (m, 2H), 7.45 ~ 7.28 (m, 4H), 7.11 (s, 1H), 6.97 (d, *J* = 8.5 Hz, 3H), 6.74 (d, *J* = 8.5 Hz, 1H), 3.89 (s, 3H), 3.77 (s, 3H), 3.68 (s, 3H). <sup>13</sup>C NMR (101 MHz, CDCl<sub>3</sub>) δ: 188.12 (s), 165.75 (s), 156.37(s), 156.26 (s), 140.05 (s), 130.95 (s), 130.88 (s), 129.74 (s), 129.66 (s), 127.89 (s), 125.37 (s), 125.28 (s), 123.78 (s), 123.64 (s), 121.86 (s), 114.67 (s), 114.59 (s), 112.64 (s), 112.38 (s), 110.56 (d, *J* = 11.7 Hz), 56.68 (d, *J* = 9.3 Hz), 54.37 (s). IR (KBr, ν, cm<sup>-1</sup>): 3413, 3297, 3063, 2941, 1708, 1651, 1549, 1507, 1478, 1369, 1280, 1194, 1141, 1029, 966, 932, 898, 829, 750, 698, 496. MS (ESI) *m/z*: 454.1 (M<sup>+</sup>), calculated MS 454.11.

#### 4.3.3(*E*)-2-(3-(4-Bromophenyl)-3-oxoprop-1-enyl)phenyl-3,4-dimethoxybenzenesulfonate (3b)

m.p. 155-157 °C. <sup>1</sup>H NMR (500 MHz, CDCl<sub>3</sub>) δ 7.80 (d, *J* = 8.4 Hz, 2H), 7.72 ~ 7.57 (m, 4H), 7.57 ~ 7.27 (m, 5H), 7.19 (dd, *J* = 24.5, 8.7 Hz, 2H), 6.76 (d, *J* = 8.5 Hz, 1H), 3.80 (s, 3H), 3.73 (s, 3H). <sup>13</sup>C NMR (101 MHz, CDCl<sub>3</sub>) δ: 189.16 (s), 153.27 (s), 149.79 (s), 148.36 (s), 139.87 (s), 136.69(s), 130.71 (s), 130.54(s), 129.85 (d, *J* = 6.6 Hz), 128.24 (s), 127.76 (s), 124.38 (s), 123.98 (s), 123.59 (s), 122.29 (s), 120.59 (s), 114.35 (s), 112.57 (s), 112.35 (s), 110.78 (s), 56.98 (d, *J* = 10.8 Hz). IR (KBr, ν, cm<sup>-1</sup>):

3414, 3300, 3061, 2948, 1710, 1649, 1546, 1505, 1480, 1374, 1283, 1191, 1143, 1030, 969, 931, 898, 826, 750, 698, 496. MS (ESI)  $m/z$ : 502.1 ( $M^+$ ), calculated MS 502.01.

#### 4.3.4(*E*)-2-(3-(4-Nitrophenyl)-3-oxoprop-1-enyl)phenyl-3,4-dimethoxybenzenesulfonate (4b)

m.p. 145-147 °C.  $^1\text{H}$  NMR (400 MHz,  $\text{CDCl}_3$ )  $\delta$  7.62 (dd,  $J = 7.8, 1.5$  Hz, 1H), 7.49 ~ 7.28 (m, 9H), 7.18 (d,  $J = 2.1$  Hz, 1H), 6.95 (d,  $J = 16.1$  Hz, 1H), 6.83 (d,  $J = 8.6$  Hz, 1H), 3.88 (s, 3H), 3.85 (s, 3H).  $^{13}\text{C}$  NMR (101 MHz,  $\text{CDCl}_3$ )  $\delta$ : 187.37 (s), 151.88 (s), 151.32 (d,  $J = 7.5$  Hz), 149.63 (s), 143.27 (s), 140.59 (s), 130.76 (s), 130.37 (s), 128.79 (s), 127.66 (s), 124.35 (s), 124.09 (s), 121.68 (s), 120.92 (s), 120.65 (s), 114.37 (s), 112.57 (s), 88.93 (s), 88.05 (s), 87.88 (s), 54.06 (d,  $J = 12.1$  Hz). IR (KBr,  $\nu$ ,  $\text{cm}^{-1}$ ): 3411, 3296, 3062, 2947, 1706, 1651, 1548, 1506, 1480, 1371, 1283, 1195, 1146, 1024, 969, 932, 898, 829, 751, 698, 496. MS (ESI)  $m/z$ : 469.1 ( $M^+$ ), calculated MS 469.08.

#### 4.3.5(*E*)-2-(3-(4-Chlorophenyl)-3-oxoprop-1-enyl)phenyl-3,4-dimethoxybenzenesulfonate (5b)

m.p. 155 - 158 °C.  $^1\text{H}$  NMR (400 MHz,  $\text{CDCl}_3$ )  $\delta$  7.92 – 7.85 (m, 2H), 7.60 (dd,  $J = 8.7, 7.4$  Hz, 2H), 7.52 ~ 7.32 (m, 6H), 7.17 (dd,  $J = 16.1, 9.0$  Hz, 2H), 6.76 (d,  $J = 8.6$  Hz, 1H), 3.81 (s, 3H), 3.72 (s, 3H).  $^{13}\text{C}$  NMR (101 MHz,  $\text{CDCl}_3$ )  $\delta$ : 187.05 (s), 152.85 (s), 151.62 (s), 148.96 (s), 140.83 (s), 138.27 (s), 135.72 (s), 128.77 (d,  $J = 6.2$  Hz), 126.88 (s), 126.29 (d,  $J = 7.3$  Hz), 125.75 (s), 124.79 (s), 124.64 (s), 121.39 (s), 120.54 (s), 115.79 (s), 115.03 (s), 99.07 (s), 98.65 (s), 56.97 (d,  $J = 10.85$  Hz). IR (KBr,  $\nu$ ,  $\text{cm}^{-1}$ ): 3415, 3300, 3064, 2942, 1711, 1653, 1546, 1512, 1483, 1370, 1283, 1190, 1139, 1031, 968, 933, 894, 829, 752, 698, 491. MS (ESI)  $m/z$ : 458.1 ( $M^+$ ), calculated MS 458.06.

#### 4.3.6(*E*)-2-(3-(3,4-Dichlorophenyl)-3-oxoprop-1-enyl)phenyl-3,4-dimethoxybenzenesulfonate (6b)

m.p. 180 - 182 °C.  $^1\text{H}$  NMR (400 MHz,  $\text{CDCl}_3$ )  $\delta$  8.04 (t,  $J = 1.7$  Hz, 1H), 7.85 (d,  $J = 7.8$  Hz, 1H), 7.72 (d,  $J = 8.8$  Hz, 1H), 7.61 (dd,  $J = 8.6, 7.3$  Hz, 2H), 7.44 (dd,  $J = 8.1, 1.4$  Hz, 1H), 7.40 (d,  $J = 7.8$  Hz, 1H), 7.35 (ddd,  $J = 8.6, 5.3, 2.5$  Hz, 2H), 7.16 (dd,  $J = 8.9, 6.8$  Hz, 2H), 6.76 (d,  $J = 8.6$  Hz, 1H), 3.81 (s, 3H), 3.74 (s, 3H).  $^{13}\text{C}$

NMR (100 MHz, CDCl<sub>3</sub>)  $\delta$ : 188.02(s), 153.57 (s), 150.73 (s), 148.59 (s), 139.62 (s), 137.37 (s), 136.93 (s), 136.01 (s), 135.49 (s), 135.27 (s), 133.38 (s), 131.89 (s), 129.18 (s), 121.07 (s), 117.27 (s), 117.08 (s), 114.71 (s), 110.34 (s), 78.53 (s), 77.65 (s), 77.39 (s), 56.29 (d,  $J = 9,7$  Hz). IR (KBr,  $\nu$ , cm<sup>-1</sup>): 3410, 3296, 3064, 2942, 1714, 1653, 1542, 1512, 14783, 1375, 1279, 1190, 1138, 1029, 966, 935, 892, 829, 750, 694, 498. MS (ESI)  $m/z$ : 492.0 (M<sup>+</sup>), calculated MS 492.02.

#### 4.3.7(*E*)-2-(3-(3,4-Dimethylphenyl)-3-oxoprop-1-enyl)phenyl-3,4-dimethoxybenzenesulfonate (7b)

m.p. 210-213 °C. <sup>1</sup>H NMR (400 MHz, CDCl<sub>3</sub>)  $\delta$  7.79 ~ 7.29 (m, 9H), 7.22 (d,  $J = 11.6$  Hz, 1H), 7.11 (d,  $J = 2.1$  Hz, 1H), 6.74 (d,  $J = 8.6$  Hz, 1H), 3.77 (s, 3H), 3.69 (s, 3H), 2.35 (s, 6H). <sup>13</sup>C NMR (100 MHz, CDCl<sub>3</sub>)  $\delta$ : 188.32 (s), 151.76 (s), 150.37 (s), 148.41 (s), 140.23 (s), 140.11 (s), 135.71 (s), 134.28 (s), 130.94 (s), 130.81 (s), 128.59 (s), 128.17 (s), 127.25 (s), 121.68 (s), 120.37 (d,  $J = 4.6$  Hz), 118.83 (s), 113.78 (s), 112.49 (s), 112.05 (s), 110.57 (s), 56.72 (d,  $J = 6.7$  Hz), 18.18 (s), 18.07 (s). IR (KBr,  $\nu$ , cm<sup>-1</sup>): 3415, 3296, 3066, 2938, 1712, 1655, 1553, 1512, 1483, 1375, 1287, 1196, 1144, 1030, 969, 933, 898, 825, 736, 693, 499. MS (ESI)  $m/z$ : 452.1 (M<sup>+</sup>), calculated MS 452.13.

#### 4.3.8(*E*)-2-(3-Oxo-3-*o*-tolylprop-1-enyl)phenyl-3,4-dimethoxybenzenesulfonate (8b)

m.p. 170-172 °C. <sup>1</sup>H NMR (400 MHz, CDCl<sub>3</sub>)  $\delta$  7.61 (dd,  $J = 7.7, 1.2$  Hz, 1H), 7.48 ~ 7.37 (m, 4H), 7.36 – 7.26 (m, 5H), 7.15 (d,  $J = 2.1$  Hz, 1H), 6.97 (d,  $J = 16.1$  Hz, 1H), 6.80 (d,  $J = 8.6$  Hz, 1H), 3.82 (d,  $J = 11.9$  Hz, 6H), 2.44 (s, 3H). <sup>13</sup>C NMR (100 MHz, CDCl<sub>3</sub>)  $\delta$ : 189.87 (s), 151.27 (s), 150.28 (s), 148.33 (s), 142.29 (s), 138.87 (s), 133.79 (s), 133.24 (s), 130.64 (s), 130.07 (s), 128.53 (s), 126.81 (s), 125.59 (s), 124.76 (s), 124.27 (s), 124.06 (s), 121.08 (s), 120.54(s), 114.07 (d,  $J = 6.9$  Hz), 110.58 (s), 56.73 (d,  $J = 11.3$  Hz), 18.11(s). IR (KBr,  $\nu$ , cm<sup>-1</sup>): 3414, 3301, 3063, 2947, 1711, 1652, 1548, 1510, 1483, 1376, 1283, 1194, 1143, 1026, 969, 936, 894, 826, 751, 696, 496. MS (ESI)  $m/z$ : 438.1 (M<sup>+</sup>), calculated MS 438.11.

#### 4.3.9(*E*)-2-(3-(2-Nitrophenyl)-3-oxoprop-1-enyl)phenyl-3,4-dimethoxybenzenesulfonate (9b)

m.p. 197-198 °C.  $^1\text{H}$  NMR (400 MHz,  $\text{CDCl}_3$ )  $\delta$  7.71 (d,  $J = 7.6$  Hz, 1H), 7.54 ~ 7.34 (m, 6H), 7.24 (dd,  $J = 8.5, 2.2$  Hz, 1H), 7.04 (d,  $J = 2.1$  Hz, 1H), 6.99 ~ 6.90 (m, 2H), 6.62 (d,  $J = 8.6$  Hz, 1H), 6.34 (s, 1H), 3.69 (s, 3H), 3.60 (s, 3H).  $^{13}\text{C}$  NMR (100 MHz,  $\text{CDCl}_3$ )  $\delta$ : 187.35 (s), 153.27 (s), 151.78 (s), 151.39 (s), 150.27 (s), 140.26 (s), 136.19 (s), 136.08 (s), 130.79 (s), 130.63 (s), 127.57 (s), 127.28 (s), 123.68 (s), 123.21 (s), 122.54 (s), 120.77 (s), 120.32 (s), 114.67 (s), 114.29 (s), 110.58 (s), 110.23 (s), 56.91 (d,  $J = 12.8$  Hz). IR (KBr,  $\nu$ ,  $\text{cm}^{-1}$ ): 3416, 3298, 3068, 2942, 1714, 1658, 1546, 1506, 1484, 1378, 1290, 1185, 1144, 1035, 968, 934, 896, 822, 754, 695, 494. MS (ESI)  $m/z$ : 469.1 ( $\text{M}^+$ ), calculated MS 469.08.

#### 4.3.10(*E*)-2-(3-(4-Ethoxyphenyl)-3-oxoprop-1-enyl)phenyl-3,4-dimethoxybenzene sulfonate (10b)

m.p. 145-147 °C.  $^1\text{H}$  NMR (400 MHz,  $\text{CDCl}_3$ )  $\delta$  8.04 ~ 7.93 (m, 2H), 7.63 (dd,  $J = 15.1, 11.7$  Hz, 2H), 7.51 ~ 7.47 (m, 2H), 7.42 (dt,  $J = 7.0, 3.5$  Hz, 2H), 7.31 (d,  $J = 6.3$  Hz, 1H), 7.16 (d,  $J = 2.2$  Hz, 1H), 7.06 ~ 6.96 (m, 2H), 6.79 (d,  $J = 8.6$  Hz, 1H), 4.18 (q,  $J = 7.0$  Hz, 2H), 3.83 (s, 3H), 3.73 (s, 3H), 1.51 (t,  $J = 7.0$  Hz, 3H).  $^{13}\text{C}$  NMR (101 MHz,  $\text{CDCl}_3$ )  $\delta$  187.64 (s), 163.02 (s), 153.98 (s), 149.19 (s), 148.39 (s), 136.45 (s), 131.16 (s), 130.83 (s), 130.49 (s), 129.37 (s), 127.79 (s), 127.43 (s), 125.72 (s), 124.29 (s), 123.62 (s), 123.08 (s), 114.34 (s), 110.46 (d,  $J = 7.9$  Hz), 77.39 (s), 77.08 (s), 76.76 (s), 56.09 (d,  $J = 16.6$  Hz), 14.74 (s). IR (KBr,  $\nu$ ,  $\text{cm}^{-1}$ ): 3414, 3302, 3062, 2948, 1712, 1656, 1549, 1512, 1482, 1376, 1283, 1195, 1143, 1032, 972, 935, 899, 825, 753, 699, 496. MS (ESI)  $m/z$ : 468.1 ( $\text{M}^+$ ), calculated MS 468.12.

#### 4.3.11(*E*)-2-(3-(4-Fluorophenyl)-3-oxoprop-1-enyl)phenyl-3,4-dimethoxybenzenesulfonate (11b)

m.p. 165-167 °C.  $^1\text{H}$  NMR (400 MHz,  $\text{CDCl}_3$ )  $\delta$  8.01 – 7.94 (m, 2H), 7.65 – 7.55 (m, 2H), 7.50 – 7.28 (m, 4H), 7.23 – 7.11 (m, 4H), 6.76 (d,  $J = 8.6$  Hz, 1H), 3.80 (s, 3H), 3.71 (s, 3H).  $^{13}\text{C}$  NMR (100 MHz,  $\text{CDCl}_3$ )  $\delta$  189.12 (s), 165.31 (s), 151.27 (s), 149.91 (d,  $J = 4.8$  Hz), 149.63 (s), 140.51 (s), 131.78 (d,  $J = 6.2$  Hz), 128.76 (s), 128.37 (s), 127.61 (s), 127.59 (s), 123.07 (s), 120.87 (s), 116.20 (s), 115.88 (s), 115.76 (s), 115.23 (d,  $J = 12.7$  Hz), 113.82 (s), 57.29 (s). IR (KBr,  $\nu$ ,  $\text{cm}^{-1}$ ): 3414, 3294, 3066, 2948, 1713, 1653, 1549, 1503, 1483, 1376, 1285, 1196, 1145, 1022, 968, 933, 894, 822, 756, 699, 498. MS (ESI)  $m/z$ : 442.1 ( $\text{M}^+$ ), calculated MS 442.09.

**4.3.12(E)-2-(3-(3-Methoxyphenyl)-3-oxoprop-1-enyl)phenyl-3,4-dimethoxybenzene sulfonate (12b)**

m.p. 160-162 °C. <sup>1</sup>H NMR (400 MHz, CDCl<sub>3</sub>) δ 7.60 (dd, *J* = 11.3, 9.4 Hz, 2H), 7.51 ~ 7.29 (m, 7H), 7.25 – 7.17 (m, 1H), 7.17 ~ 7.08 (m, 2H), 6.74 (d, *J* = 8.6 Hz, 1H), 3.89 (s, 3H), 3.78 (s, 3H), 3.70 (s, 3H). <sup>13</sup>C NMR (100 MHz, CDCl<sub>3</sub>) δ: 187.79 (s), 156.74 (s), 151.57 (s), 149.94 (s), 149.71(s), 140.23 (s), 133.25 (s), 132.74 (s), 130.57 (s), 130.24 (s), 123.71 (s), 123.38(s), 120.89 (s), 117.58 (s), 117.43 (s), 110.44 (d, *J* = 9.2 Hz), 107.53 (s), 107.23 (s), 106.83 (s), 104.83 (s), 56.12 (d, *J* = 8.9 Hz), 55.92 (s). IR (KBr, ν, cm<sup>-1</sup>): 3414, 3302, 3062, 2945, 1712, 1655, 1548, 1512, 1482, 1378, 1288, 1196, 1139, 1032, 970, 933, 898, 834, 752, 698, 496. MS (ESI) *m/z*: 454.1 (M<sup>+</sup>), calculated MS 454.11.

**4.3.13(E)-2-(3-(2-Chlorophenyl)-3-oxoprop-1-enyl)phenyl-3,4-dimethoxybenzene sulfonate (13b)**

m.p. 176-178°C. <sup>1</sup>H NMR (400 MHz, CDCl<sub>3</sub>) δ 7.62 (dd, *J* = 7.8, 1.5 Hz, 1H), 7.49 ~ 7.28 (m, 9H), 7.18 (d, *J* = 2.1 Hz, 1H), 6.95 (d, *J* = 16.1 Hz, 1H), 6.83 (d, *J* = 8.6 Hz, 1H), 3.88 (s, 3H), 3.85 (s, 3H). <sup>13</sup>C NMR (100 MHz, CDCl<sub>3</sub>) δ: 189.74(s), 152.07 (s), 150.39 (s), 150.29 (s), 143.37 (s), 136.92 (s), 136.58 (s), 130.06 (s), 129.91 (s), 129.27 (s), 128.35(s), 127.33 (s), 127.18 (s), 126.64 (s), 123.28 (s), 123.17(s), 118.15 (s), 117.83(s), 112.89 (s), 110.27 (s), 110.16 (s), 56.64 (d, *J* = 12.4 Hz). IR (KBr, ν, cm<sup>-1</sup>): 3416, 3296, 3066, 2942, 1713, 1655, 1544, 1510, 1482, 1376, 1280, 1188, 1139, 1026, 963, 928, 893, 824, 744, 695, 493. MS (ESI) *m/z*: 458.1 (M<sup>+</sup>), calculated MS 458.06.

**4.3.14(E)-2-(3-(3-Bromophenyl)-3-oxoprop-1-enyl)phenyl-3,4-dimethoxybenzene sulfonate (14b)**

m.p. 181-184 °C. <sup>1</sup>H NMR (400 MHz, CDCl<sub>3</sub>) δ 8.00 (d, *J* = 2.0 Hz, 1H), 7.77 (dd, *J* = 8.3, 2.0 Hz, 1H), 7.62 (ddd, *J* = 17.7, 9.8, 6.3 Hz, 3H), 7.47 ~ 7.44 (m, 1H), 7.39 (dd, *J* = 8.2, 1.1 Hz, 1H), 7.37 ~ 7.32 (m, 2H), 7.17 (dd, *J* = 11.2, 9.0 Hz, 2H), 3.83 (s, 3H), 3.77 (s, 3H). <sup>13</sup>C NMR (100 MHz, CDCl<sub>3</sub>) δ: 188.15 (s), 153.09 (s), 151.76 (s), 151.54 (s), 140.38 (s), 140.12 (s), 136.28 (s), 129.75 (s), 129.63 (s), 127.18 (s), 127.01(s), 123.29 (s), 122.98 (s), 122.14 (s), 117.15 (d, *J* = 5.6 Hz), 117.09 (s),

110.87 (s), 110.66 (s), 108.57 (s), 104.38 (s), 57.26 (s), 57.19 (s). IR (KBr,  $\nu$ ,  $\text{cm}^{-1}$ ): 3416, 3300, 3068, 2942, 1714, 1656, 1552, 1513, 1482, 1376, 1285, 1194, 1145, 1032, 962, 935, 892, 825, 744, 698, 499. MS (ESI)  $m/z$ : 502.1 ( $\text{M}^+$ ), calculated MS 502.01.

#### **4.3.15(E)-2-(3-(3-Fluorophenyl)-3-oxoprop-1-enyl)phenyl-3,4-dimethoxybenzenesulfonate (15b)**

m.p. 167-168 °C.  $^1\text{H}$  NMR (400 MHz,  $\text{CDCl}_3$ )  $\delta$  7.71 (d,  $J = 7.8$  Hz, 1H), 7.65 ~ 7.58 (m, 3H), 7.46 (ddt,  $J = 13.4, 8.1, 6.2$  Hz, 3H), 7.33 (ddd,  $J = 10.2, 8.5, 2.1$  Hz, 3H), 7.21 ~ 7.14 (m, 2H), 6.77 (d,  $J = 8.6$  Hz, 1H), 3.80 (s, 3H), 3.73 (s, 3H).  $^{13}\text{C}$  NMR (100 MHz,  $\text{CDCl}_3$ )  $\delta$ : 189.12 (s), 167.53 (s), 152.79 (s), 149.81 (s), 149.62 (s), 142.17 (s), 140.87 (s), 131.95 (s), 130.27 (s), 129.85 (s), 124.35 (s), 124.21 (s), 122.35 (s), 121.28 (s), 120.84 (s), 120.77 (s), 114.64 (d,  $J = 10.3$  Hz), 112.88 (s), 112.53 (s), 112.09 (s), 56.87 (d,  $J = 13.9$  Hz). IR (KBr,  $\nu$ ,  $\text{cm}^{-1}$ ): 3409, 3295, 3065, 2940, 1713, 1656, 1543, 1511, 1482, 1370, 1279, 1190, 1139, 1026, 964, 932, 894, 832, 752, 688, 496. MS (ESI)  $m/z$ : 442.1 ( $\text{M}^+$ ), calculated MS 442.08.

#### **4.3.16(E)-2-(3-(2,4-Dimethylphenyl)-3-oxoprop-1-enyl)-phenyl-3,4-dimethoxybenzenesulfonate (16b)**

m.p. 160-163 °C.  $^1\text{H}$  NMR (400 MHz,  $\text{CDCl}_3$ )  $\delta$  7.71 (d,  $J = 7.8$  Hz, 1H), 7.65 ~ 7.58 (m, 3H), 7.46 (ddt,  $J = 13.4, 8.1, 6.2$  Hz, 3H), 7.33 (ddd,  $J = 10.2, 8.5, 2.1$  Hz, 3H), 7.21 ~ 7.14 (m, 2H), 6.77 (d,  $J = 8.6$  Hz, 1H), 3.80 (s, 3H), 3.73 (s, 3H).  $^{13}\text{C}$  NMR (100 MHz,  $\text{CDCl}_3$ )  $\delta$ : 191.76 (s), 152.06 (s), 151.87 (s), 151.64 (s), 142.39 (s), 141.82 (s), 141.08 (s), 132.79 (s), 132.15 (s), 131.28 (s), 129.51 (s), 129.27 (s), 124.28 (s), 123.89 (s), 118.54 (s), 118.33 (s), 114.88 (s), 114.29 (s), 113.07 (s), 89.39 (s), 88.76 (s), 56.25 (d,  $J = 11.4$  Hz), 20.05 (s), 19.58 (s). IR (KBr,  $\nu$ ,  $\text{cm}^{-1}$ ): 3414, 3296, 3058, 2940, 1706, 1648, 1546, 1503, 1482, 1368, 1279, 1190, 1138, 1022, 966, 936, 894, 822, 749, 694, 492. MS (ESI)  $m/z$ : 452.1 ( $\text{M}^+$ ), calculated MS 452.13.

#### **4.3.17(E)-2-(3-Oxo-3-phenylprop-1-enyl)phenyl-3,4-dimethoxybenzenesulfonate (17b)**

m.p. 144-146 °C.  $^1\text{H}$  NMR (400 MHz,  $\text{CDCl}_3$ )  $\delta$  8.00 ~ 7.89 (m, 2H), 7.58 (dd,  $J = 7.8, 4.8$  Hz, 2H), 7.56 ~ 7.46 (m, 4H), 7.35 (ddd,  $J = 8.5, 4.6, 2.2$  Hz, 3H), 7.25 ~ 7.14 (m, 2H), 6.74 (d,  $J = 8.6$  Hz, 1H), 3.83 (s, 3H), 3.67 (s, 3H).  $^{13}\text{C}$  NMR (100 MHz,

CDCl<sub>3</sub>)  $\delta$ : 188.29 (s), 152.15 (s), 149.87 (s), 149.56 (s), 140.28 (s), 136.36 (s), 135.71 (s), 132.28 (s), 131.99 (s), 131.83 (s), 128.21 (d,  $J = 12.2$  Hz), 127.62 (s), 123.88 (s), 123.57 (s), 120.20 (s), 118.58 (s), 115.75 (s), 115.52 (s), 114.31 (s), 110.89 (s), 56.05 (d,  $J = 6.9$  Hz). IR (KBr,  $\nu$ , cm<sup>-1</sup>): 3416, 3295, 3066, 2940, 1712, 1656, 1543, 1512, 1482, 1370, 1286, 1190, 1132, 1033, 969, 936, 899, 824, 752, 696, 493. MS (ESI)  $m/z$ : 424.1 (M<sup>+</sup>), calculated MS 424.10.

#### 4.3.18(*E*)-4-Chloro-2-(3-oxo-3-phenylprop-1-enyl)phenyl-3,4-dimethoxybenzenesulfonate (18b)

m.p. 169-171 °C. <sup>1</sup>H NMR (500 MHz, CDCl<sub>3</sub>)  $\delta$  7.80 (d,  $J = 8.4$  Hz, 2H), 7.66 ~ 7.61 (m, 3H), 7.48 ~ 7.30 (m, 5H), 7.22 ~ 7.14 (m, 2H), 6.76 (d,  $J = 8.5$  Hz, 1H), 3.80 (s, 3H), 3.73 (s, 3H). <sup>13</sup>C NMR (100 MHz, CDCl<sub>3</sub>)  $\delta$ : 187.58 (s), 151.87 (s), 149.47 (s), 149.03 (s), 146.37 (s), 140.27 (s), 136.81 (s), 135.12 (s), 130.59 (s), 129.27 (s), 129.03 (s), 128.14 (s), 126.19 (s), 125.83 (s), 125.35 (s), 124.12 (d,  $J = 5.3$  Hz), 120.09 (s), 115.58 (s), 115.12 (s), 112.39 (s), 56.91 (s), 55.87 (s). IR (KBr,  $\nu$ , cm<sup>-1</sup>): 3416, 3305, 3058, 2944, 1713, 1654, 1541, 1504, 1482, 1376, 1278, 1188, 1138, 1033, 966, 928, 896, 826, 752, 694, 491. MS (ESI)  $m/z$ : 458.1 (M<sup>+</sup>), calculated MS 458.06.

#### 4.3.19(*E*)-2,4-Dichloro-6-(3-oxo-3-phenylprop-1-enyl)phenyl-3,4-dimethoxybenzenesulfonate (19b)

m.p. 170-173 °C. <sup>1</sup>H NMR (400 MHz, CDCl<sub>3</sub>)  $\delta$  7.98 ~ 7.90 (m, 2H), 7.53 (dt,  $J = 15.0, 7.7$  Hz, 4H), 7.42 ~ 7.28 (m, 3H), 7.17 (dd,  $J = 26.8, 9.0$  Hz, 2H), 6.74 (d,  $J = 8.6$  Hz, 1H), 3.80 (s, 3H), 3.68 (s, 3H). <sup>13</sup>C NMR (100 MHz, CDCl<sub>3</sub>)  $\delta$ : 187.32 (s), 153.45 (s), 153.37 (s), 149.27 (s), 142.07 (s), 135.87 (s), 133.76 (s), 130.84 (s), 128.71 (s), 128.67 (s), 128.39 (d,  $J = 4.8$  Hz), 124.12 (s), 124.07 (s), 122.29 (s), 121.73 (s), 121.01 (s), 119.83 (s), 115.35 (s), 115.27 (s), 110.79 (s), 55.28 (s), 54.02 (s). IR (KBr,  $\nu$ , cm<sup>-1</sup>): 3410, 3296, 3062, 2940, 1703, 1644, 1542, 1500, 1472, 1370, 1279, 1189, 1138, 1024, 960, 933, 890, 822, 752, 695, 491. MS (ESI)  $m/z$ : 492.0 (M<sup>+</sup>), calculated MS 492.02.

#### 4.4 Single crystal structure determination

The crystal structure determination of compound **10b** was carried out on a Nonius CAD4 diffractometer equipped with graphite-monochromated MoK $\alpha$  ( $\lambda$  0.7103 Å)

radiation (Figure 8). The structure was solved by direct methods and refined on  $F^2$  by full-matrix least-squares methods using SHELX-97<sup>24</sup>. All non-hydrogen atoms were refined anisotropically. All hydrogen atoms were placed in the calculated positions and were assigned fixed isotropic thermal parameters at 1.2 times the equivalent isotropic U of the atoms to which they are attached and allowed to ride on their respective parent atoms. The contributions of these hydrogen atoms were included in the structure-factors calculations. The crystal data, data collection, and refinement parameter for the compound **10b** are listed in Table 4.

#### 4.5 Antiproliferation assay and tubulin polymerization inhibition

The antiproliferative activity of the prepared compounds against MCF-7, HeLa, Hep G2, HCT-116 carcinoma cell lines were evaluated as described elsewhere with some modifications. Target tumor cell lines were grown to log phase in RPMI 1640 medium supplemented with 10% fetal bovine serum. After diluting to  $2 \times 10^4$  cells  $\text{mL}^{-1}$  with the complete medium, 100  $\mu\text{L}$  of the obtained cell suspension was added to each well of 96-well culture plates. The subsequent incubation was permitted at 37 °C, 5%  $\text{CO}_2$  atmosphere for 24 h before the cytotoxicity assessments. Tested samples at pre-set concentrations were added to six wells with colchicine coassayed as positive references. After 48 h exposure period, 40  $\mu\text{L}$  of PBS containing 2.5 mg/mL of MTT (3-(4,5-dimethylthiazol-2-yl)-2,5-diphenyltetrazolium bromide) was added to each well. Four hours later, 100  $\mu\text{L}$  extraction solution (10% SDS - 5% isobutyl alcohol - 0.01 M HCl) was added. After an overnight incubation at 37 °C, the optical density was measured at a wavelength of 570 nm on an ELISA microplate reader. In all experiments three replicate wells were used for each drug concentration. Each assay was carried out for at least three times. The results were summarized in Table 2.

The effects on tubulin polymerization of compound **10b** and positive control CA-4 were evaluated as  $\text{IC}_{50}$  values showed in Table 3. In this research the methodologies were as reported previously in our lab<sup>14</sup>. Concentrations of gradients were pre-incubated with purified bovine brain tubulin (10  $\mu\text{M}$ ) in glutamate buffer in 30 °C.

Then they were cooled to 0 °C, after the addition of GTP, and transportation in spectrophotometer in 30 °C, the assembly of tubulin was observed turbidimetrically for 50% after 30min incubation.

#### 4.6 Apoptosis morphological assessment by fluorescent DAPI staining

After MCF-7 cells were grown on coverglass-bottom concfal dish and incubated with compound **10b** at gradient concentrations of 0, 50 nM, 100 nM and 200 nM in DMEM media for 24 hours at 37 °C<sup>15</sup>. The media was removed and cells were washed with 4,6-Diaminido-2-phenylindole staining solution (DAPI, 10 µg/mL) staining solution three times. Then, cells were added DAPI staining solution 500 µL for each dish for 15 min. Before scanned under microscopy, the staining solution was removed and the dishes were washed with methanol for three times, then glycerin was added on the dishes for imaging. All imaging experiments were performed on a fixed cell DSU spinning confocal microscope (Olympus). Excitation and emission monitored used Alexa Fluor 568 filters. Imaging performed using X40 objective, and captured using Slidebook software. The result was shown in Figure. 2.

#### 4.7 Flow cytometry on apoptosis and cell cycle

Cells ( $1.3 \times 10^5$  cells/mL) were cultured in the presence or not of benzenesulfonate derivatives at 0, 50nM, 100nM, 200nM. After treatment for 24hours, cells were washed and fixed in PBS/ethanol (30/70). For cytofluorometric examination, cells ( $10^4$  cells/mL) were incubated for 30 min in PBS/ Triton X100, 0.2% /EDTA (1 mM), and propidium iodide (PI) (50 µg/mL) in PBS supplemented by RNase (0.5 mg/mL). The number of cells in different phases of the cell cycle was determined, and the percentage of apoptotic cells was quantified. Analyses were accomplished by a FACS Calibur (Becton Dickinson, Le Pont de Claix, France). Cell Quest software was used for data acquisition and analysis. The results were presented as in Figure 3.

Approximately  $10^5$  cells/well were plated in 6-well plates and allowed to adhere. After 12 hours, the medium was replaced with fresh culture medium containing

compounds **10b** at final concentrations of 25 nM, 50 nM, 100 nM and 200 nM. Nontreated wells received an equivalent volume of ethanol (<0.1%). After 36 h, Cells in the supernatant and adherent cells were collected using 0.25% Trypsin, 0.02% EDTA. Cells were washed with PBS and were fixed in 70% ethanol, centrifuged for 1 min at 3000 g at 4 °C, washed once with PBS buffer, treated with 1 mg/mL ribonuclease (Sigma Chemical Co.) for 15 min at 37 °C and stained with 50 mg/mL propidium iodide (Sigma Chemical Co.) for 30 min at room temperature. Flow cytometry analyses were performed on a Becton Dickinson FaCS-Calibur using the Becton Dickinson Cell Quest program. The results were summarized in Figure 4 and Figure 5.

#### 4.8 Western Blot analysis

MCF-7 cells were harvested at the indicated times, and cell pellets were frozen on dry ice before lysis. Cell pellets were lysed (25 mM HEPES, 0.1% Triton-X100, 300 mM NaCl, 20 mM  $\beta$ -glycerophosphate, 0.5 mM DTT, 1.0 mM EDTA, 1.5 mM MgCl<sub>2</sub>, pH 7.5, 0.2 mM sodium orthovanadate, and protease inhibitors). Then 100  $\mu$ g of each lysate was resolved by 10% SDS-polyacrylamide gel electrophoresis. The resolved proteins were transferred onto nitrocellulose filter paper and hybridized to the following antibodies: p-Histone H3 (Santa Cruz), histone H3 (Sigma, H0164-200UL). Quantitation of the bands was performed using Odyssey software.

#### 4.9 Molecular docking

The three-dimensional X-ray structure of microtubules crystal structure (PDB code: 1SA0) was chosen as the template for the modeling study of compound **6b** bound to colchicine-binding site. The crystal structure was obtained from the RCSB Protein Data Bank (<http://www.rcsb.org/pdb/home/home.do>). The molecular docking procedure was performed using CDOCKER protocol within Discovery Studio 3.5. For ligand preparation, the 3D structure of **6b** was generated and minimized using Discovery Studio 3.5. For protein preparation, the hydrogen atoms were added, and the water and impurities were removed. The molecular docking was performed by

inserting compound **6b** into the colchicine-binding site on microtubules on the  $\beta$  domain. Types of interactions of the docked protein with ligand-based pharmacophore model were analyzed after the end of molecular docking.

### Acknowledgement

This work was supported by the Jiangsu National Science Foundation (NO. BK2009239) and the Fundamental Research Fund for the Central Universities (NO. 1092020804).

**References:**

1. C. Dumontet and M. A. Jordan, *NAT REV DRUG DISCOV*, 2010, 9, 790-803.
2. J. Zhou and P. Giannakakou, *Current Medicinal Chemistry-Anti-Cancer Agents*, 2005, 5, 65-71.
3. J. G. White, *The American journal of pathology*, 1968, 53, 281.
4. T. L. Nguyen, C. McGrath, A. R. Hermone, J. C. Burnett, D. W. Zaharevitz, B. W. Day, P. Wipf, E. Hamel and R. Gussio, *J MED CHEM*, 2005, 48, 6107-6116.
5. C. M. Lin, H. H. Ho, G. R. Pettit and E. Hamel, *BIOCHEMISTRY-US*, 1989, 28, 6984-6991.
6. D. Simoni, R. Romagnoli, R. Baruchello, R. Rondanin, G. Grisolia, M. Eleopra, M. Rizzi, M. Tolomeo, G. Giannini and D. Alloatti, *J MED CHEM*, 2008, 51, 6211-6215.
7. D. J. Edwards, J. A. Hadfield, T. W. Wallace and S. Ducki, *ORG BIOMOL CHEM*, 2011, 9, 219-231.
8. A. Kamal, A. Viswanath, M. J. Ramaiah, J. Murty, F. Sultana, G. Ramakrishna, J. R. Tamboli, S. Pushpavalli, C. Kishor and A. Addlagatta, *MEDCHEMCOMM*, 2012, 3, 1386-1392.
9. S. L. Gwaltney, H. M. Imade, K. J. Barr, Q. Li, L. Gehrke, R. B. Credo, R. B. Warner, J. Y. Lee, P. Kovar and J. Wang, *BIOORG MED CHEM LETT*, 2001, 11, 871-874.
10. Y. Kong, K. Wang, M. C. Edler, E. Hamel, S. L. Mooberry, M. A. Paige and M. L. Brown, *BIOORGAN MED CHEM*, 2010, 18, 971-977.
11. K. V. Sashidhara, A. Kumar, M. Kumar, J. Sarkar and S. Sinha, *BIOORG MED CHEM LETT*, 2010, 20, 7205-7211.
12. D. J. Kerr, E. Hamel, M. K. Jung and B. L. Flynn, *BIOORGAN MED CHEM*, 2007, 15, 3290-3298.
13. A. Boumendjel, J. Boccard, P. Carrupt, E. Nicolle, M. Blanc, A. Geze, L. Choisnard, D. Wouessidjewe, E. Matera and C. Dumontet, *J MED CHEM*, 2008, 51, 2307-2310.
14. Y. Hu, X. Lu, K. Chen, R. Yan, Q. Li and H. Zhu, *BIOORGAN MED CHEM*, 2012, 20, 903-909.
15. Y. Qian, H. Zhang, P. Lv and H. Zhu, *BIOORGAN MED CHEM*, 2010, 18, 8218-8225.
16. O. Mazimba, I. B. Masesane and R. R. Majinda, *TETRAHEDRON LETT*, 2011, 52, 6716-6718.
17. L. M. Betts, N. C. Tam, S. H. Kabir, R. F. Langler and I. Crandall, *AUST J CHEM*, 2006, 59, 277-282.
18. Z. Junnian, X. Shuliang and C. Jiachun, *SHANGHAI J. OF IMMUNOLOGY*, 1999.
19. J. Fried, A. G. Perez and B. D. Clarkson, *The Journal of cell biology*, 1976, 71, 172-181.
20. R. B. Ravelli, B. Gigant, P. A. Curmi, I. Jourdain, S. Lachkar, A. Sobel and M. Knossow, *NATURE*, 2004, 428, 198-202.
21. J. H. Nettles, H. Li, B. Cornett, J. M. Krahn, J. P. Snyder and K. H. Downing, *SCIENCE*, 2004, 305, 866-869.
22. Y. Wei, L. Yu, J. Bowen, M. A. Gorovsky and C. D. Allis, *CELL*, 1999, 97, 99-109.
23. A. Van Hooser, D. W. Goodrich, C. D. Allis, B. R. Brinkley and M. A. Mancini, *J CELL SCI*, 1998, 111, 3497-3506.
24. G. M. Sheldrick, Göttingen, Germany, 1997.

## Figure Captions

Table 1. Structures of compounds **1b** - **19b**

Table 2. Proliferation inhibitory activities of compounds **1b** -**19b** and colchicine against cancer cells (IC<sub>50</sub> values) and cytotoxicity towards normal cells (CC<sub>50</sub> values)

Table 3. The inhibition of tubulin polymerization (IC<sub>50</sub> values)

Table 4. The crystal data, data collection, and refinement parameter for the compound **10b**

Figure 1. The structures of Colchicine and Combretastatin A4

Figure 2. The morphological changes of DAPI stained MCF-7 human breast carcinoma cells after treatment with compound **10b** (200 nM). Observed under co-focal microscope

Figure 3. Compound **10b** induced apoptosis in MCF-7 cells with the concentration of 0 (A), 50 nM (B), 100 nM (C), 200 nM (D). MCF-7 cells were treated with for 24 h.

Figure 4. Effects of **10b** on the cell cycle distribution in MCF-7 cells

Figure 5. Percentages of MCF-7 cells in each mitotic phase after treatment with compound **10b** at the concentrations of 0, 50 nM, 100 nM, 200 nM

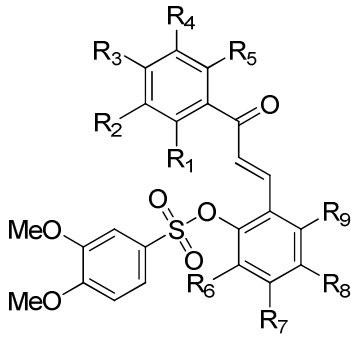
Figure 6. Binding mode of compound **6b** with microtubule (PDB code: 1SA0)

Figure 7. The docking surface of compound **6b** with microtubule (1SA0) in colchicine site

Figure 8. The crystal structure of compound **10b**

Figure 9. The Western blot analysis of phosphorylated histone (P-histone) and histone on MCF-7 cells, treated with colchicine (200 nM) and compound **10b** (200 nM)

Scheme 1. The synthesis of compounds **1b-19b**

Table 1. Structures of compounds **1b-19b**


	R <sub>1</sub>	R <sub>2</sub>	R <sub>3</sub>	R <sub>4</sub>	R <sub>5</sub>	R <sub>6</sub>	R <sub>7</sub>	R <sub>8</sub>	R <sub>9</sub>
<b>1b</b>	H	H	CH <sub>3</sub>	H	H	H	H	H	H
<b>2b</b>	H	H	OCH <sub>3</sub>	H	H	H	H	H	H
<b>3b</b>	H	H	Br	H	H	H	H	H	H
<b>4b</b>	H	H	NO <sub>2</sub>	H	H	H	H	H	H
<b>5b</b>	H	H	Cl	H	H	H	H	H	H
<b>6b</b>	H	H	Cl	Cl	H	H	H	H	H
<b>7b</b>	H	H	CH <sub>3</sub>	CH <sub>3</sub>	H	H	H	H	H
<b>8b</b>	CH <sub>3</sub>	H	H	H	H	H	H	H	H
<b>9b</b>	NO <sub>2</sub>	H	H	H	H	H	H	H	H
<b>10b</b>	H	H	OEt	H	H	H	H	H	H
<b>11b</b>	H	H	F	H	H	H	H	H	H
<b>12b</b>	H	OCH <sub>3</sub>	H	H	H	H	H	H	H
<b>13b</b>	Cl	H	H	H	H	H	H	H	H
<b>14b</b>	H	Br	H	H	H	H	H	H	H
<b>15b</b>	H	F	H	H	H	H	H	H	H
<b>16b</b>	CH <sub>3</sub>	H	CH <sub>3</sub>	H	H	H	H	H	H
<b>17b</b>	H	H	H	H	H	H	H	H	H
<b>18b</b>	H	H	H	H	H	H	H	Cl	H
<b>19b</b>	H	H	H	H	H	Cl	H	Cl	H

Table 2 Proliferation inhibitory activities of compounds **1b-19b** and colchicine against cancer cells and cytotoxicity towards normal cells.

	IC <sub>50</sub> (nM) <sup>a</sup>				CC <sub>50</sub> (nM) <sup>b</sup>
	MCF-7 <sup>c</sup>	HepG2 <sup>d</sup>	HCT-116 <sup>e</sup>	Hela <sup>f</sup>	293T <sup>g</sup>
<b>1b</b>	94.6	94.8	102.7	98.4	573.6
<b>2b</b>	83.1	82.8	106.6	99.5	460.6
<b>3b</b>	123.9	123.8	138.2	129.4	360
<b>4b</b>	110.3	114.6	122.2	125.2	387.4
<b>5b</b>	116.8	120.4	121.9	118.3	572.3
<b>6b</b>	122.3	137.9	155.4	143.5	506.6
<b>7b</b>	91.7	97.3	92.1	96.0	415.2
<b>8b</b>	99.7	96.3	95.5	100.3	574.3
<b>9b</b>	113.4	97.0	107.6	100.3	435.7
<b>10b</b>	79.2	79.2	81.34	86.8	734.8
<b>11b</b>	111.3	123.6	127.6	113.1	435.7
<b>12b</b>	107.4	102.7	98.6	106	403
<b>13b</b>	101.0	131.1	98.4	104.2	420
<b>14b</b>	144.5	157.4	144.0	137.9	541
<b>15b</b>	133.9	137.1	138.2	135.8	442.2
<b>16b</b>	90.1	85.8	86.4	90.1	434.6
<b>17b</b>	151.4	128.6	189.2	115.7	614
<b>18b</b>	149.2	116.7	124.9	164.8	841.3
<b>19b</b>	175.3	201.9	184.8	182.4	442.7
<b>colchicine</b>	150.4	123.9	125.4	131.4	797.5

<sup>a</sup> IC<sub>50</sub> values and CC<sub>50</sub> values were averaged values determined by at least two independent experiments. Variation was generally 5%.

<sup>b</sup> Minimum cytotoxic concentration required to cause a microscopically detectable alteration of normal cell morphology.

<sup>c</sup> Inhibition of MCF-7 cells' growth.

- <sup>d</sup> Inhibition of HepG2 cells' growth.
- <sup>e</sup> Inhibition of HCT-116 cells' growth.
- <sup>f</sup> Inhibition of Hela cells' growth.
- <sup>g</sup> Cytotoxicity of 293T cells' growth.

Table 3 Tubulin polymerization inhibition of Compound **10b** and positive control CA-4.

IC <sub>50</sub> values (μM) <sup>a</sup>	
Tubulin polymerization inhibition	
CA-4	3.4
Compound <b>10b</b>	12.0

<sup>a</sup>The inhibition of tubulin polymerization, N=3, variation generally 5%. Tubulin (10 μM) incubated in glutamate buffer. The IC<sub>50</sub> values were defined after 30min incubation.

Table 4 The crystal data, data collection, and refinement parameter for the compound **10b**.

compound	<b>10b</b>
Empirical formula	C <sub>25</sub> H <sub>24</sub> O <sub>7</sub> S
Molecular Weight	468.52
Temperature (K)	273(2)
Radiation	Mo-K $\alpha$ (0.7103Å)
Crystal system	Triclinic
Space group	<i>P</i> -1
a (Å)	8.5318(5)
b (Å)	10.1614(7)
c (Å)	14.1611(10)
$\alpha$ (°)	70.470(2)
$\beta$ (°)	88.224(2)
$\gamma$ (°)	87.397(2)
<i>V</i> (Å <sup>3</sup> )	1155.71(13)
<i>Z</i>	19
<i>D<sub>c</sub></i> (g cm <sup>-3</sup> )	1.667
$\mu$ (mm <sup>-1</sup> )    absort.coeff	0.948
<i>F</i> (000)	589
$\theta$ rang (deg)	2.17- 27.56
Reflections collected	12303( <i>R</i> <sub>int</sub> = 0.0270)
Indep. reflns	5177
Refns obs. [ <i>I</i> > 2 $\sigma$ ( <i>I</i> )]	4025
Data/restr./paras	5177/0/301
Goodness-of-fit on <i>F</i> <sup>2</sup>	1.053
<i>R</i> <sub>1</sub> , <i>wR</i> <sub>2</sub> (all data)	0.0622/0.1219
<i>R</i> <sub>1</sub> , <i>wR</i> <sub>2</sub> [ <i>I</i> > 2 $\sigma$ ( <i>I</i> )]	0.0444/0.0106

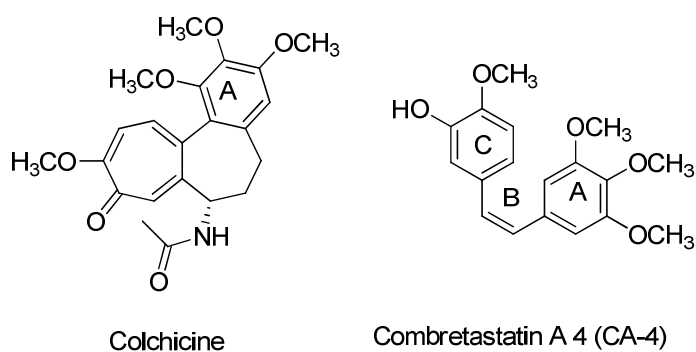


Figure 1 The structures of Colchicine and Combretastatin A 4.

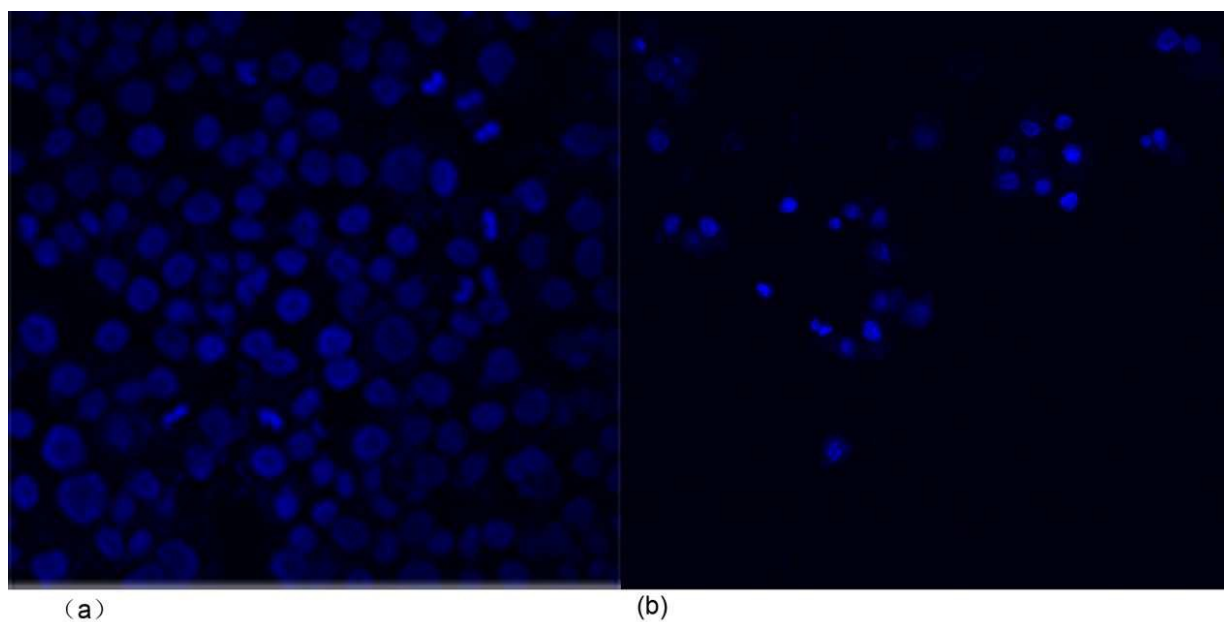


Figure 2 The morphological changes of DAPI stained MCF-7 human breast carcinoma cells after treatment with compound **10b** (200 nM). Observed under co-focal microscope. (a). MCF-7 cells treated without compound **10b**. (b). MCF-7 cells treated with the compound at 200 nM.

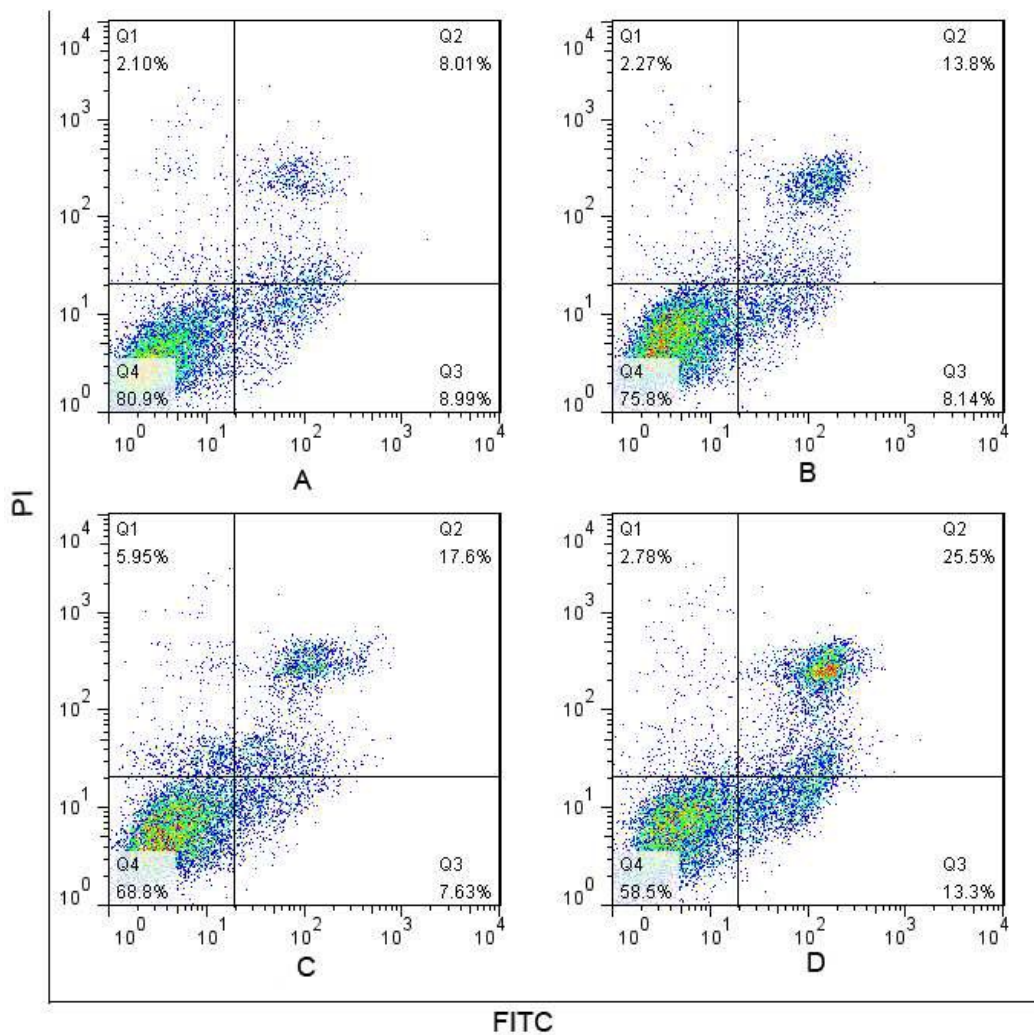


Figure 3 Compound **10b** induced apoptosis in MCF-7 cells with the concentration of 0 (A), 50 nM (B), 100 nM (C), 200 nM (D). MCF-7 cells were treated with for 24 h.

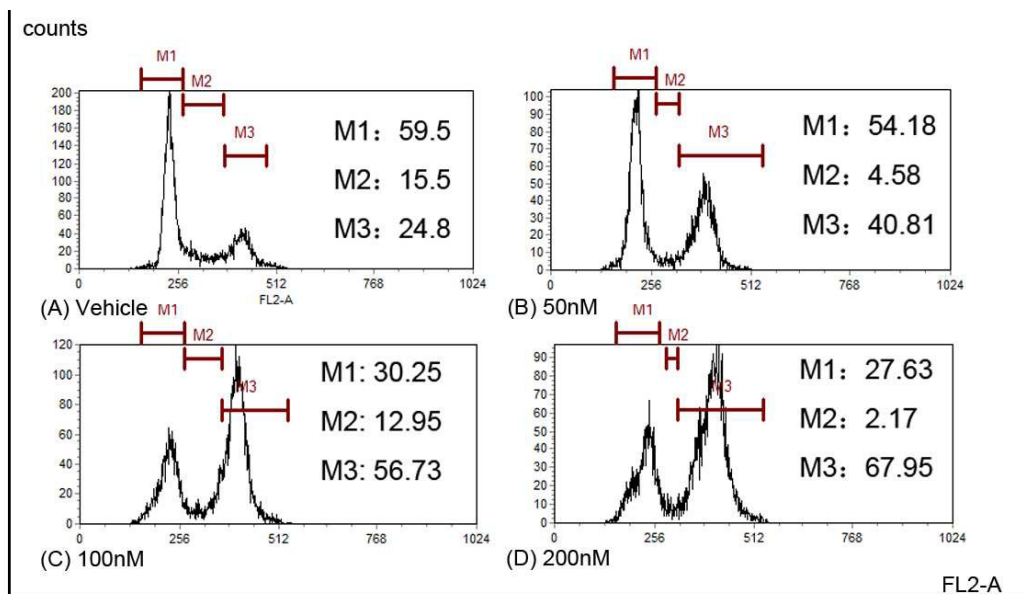


Figure 4 Effects of **10b** on the cell cycle distribution in MCF-7 cells. MCF-7 cells were treated without compound **10b** (A), 50 nM (B), 100 nM (C), 200 nM (D).

Values represent the mean  $\pm$  SD, n = 3. P < 0.05 versus control.

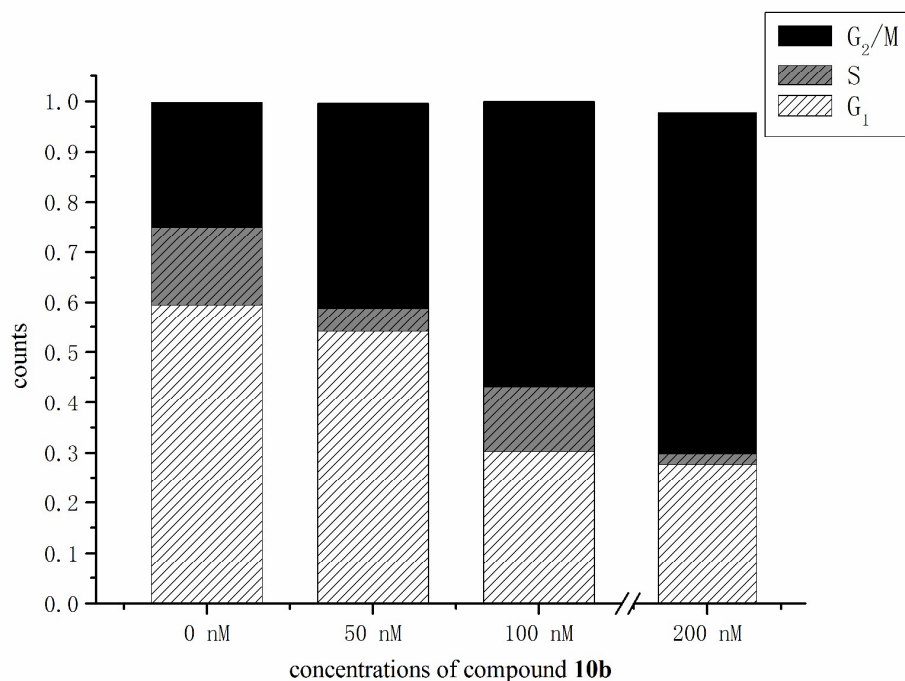


Figure 5 Percentages of MCF-7 cells in each mitotic phase after treatment with compound **10b** at the concentrations of 0, 50 nM, 100 nM, 200 nM.

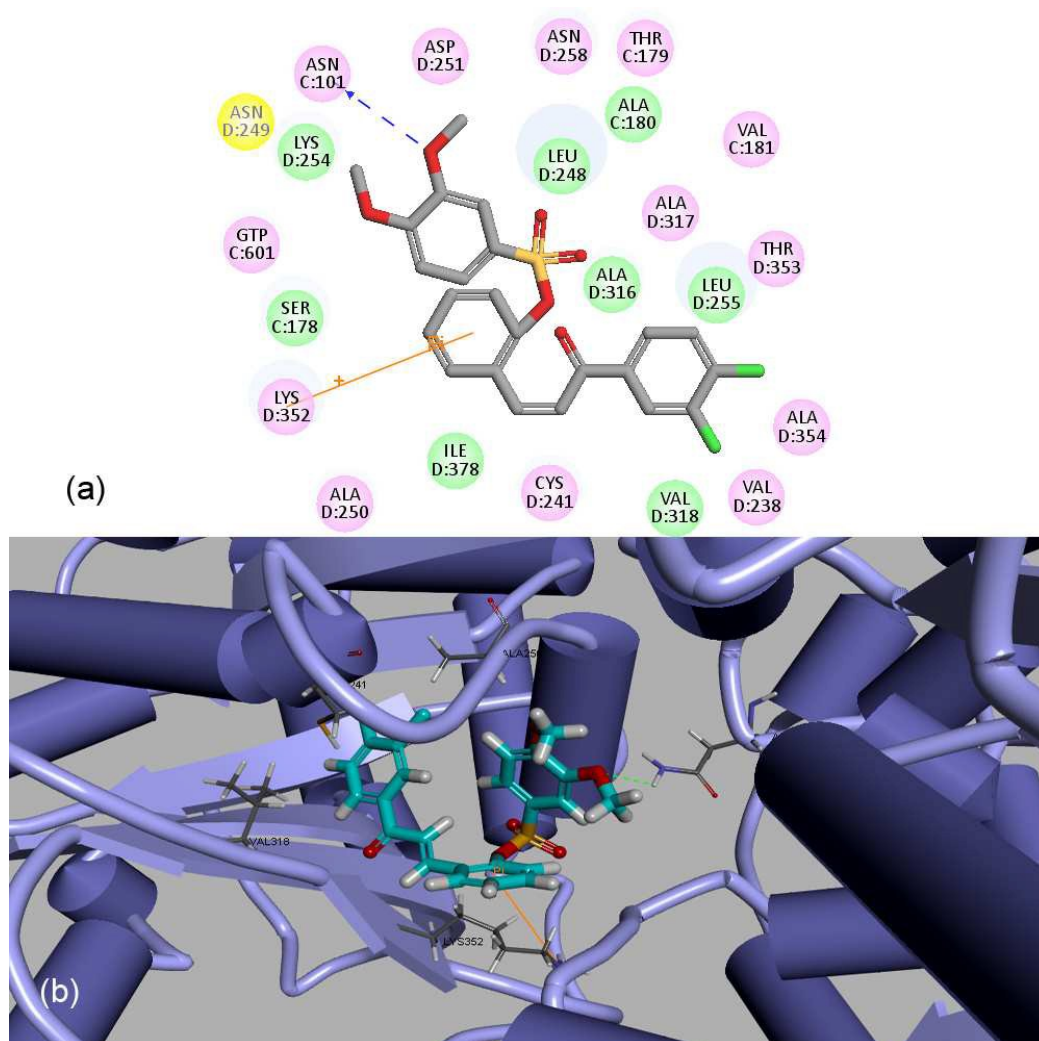


Figure 6 Binding mode of compound **6b** with microtubule (PDB code: 1SA0). (a). 2D diagram of the interaction between compound **6b** and amino acid residues of colchicine site nearby. Blue line represented hydrogen bond between benzenesulfonate ring and asn101, orange line represented pi-pi bond between chalcone moiety and lys352. (b). 3D diagram of compound **6b** inserted in microtubulin colchicine site.

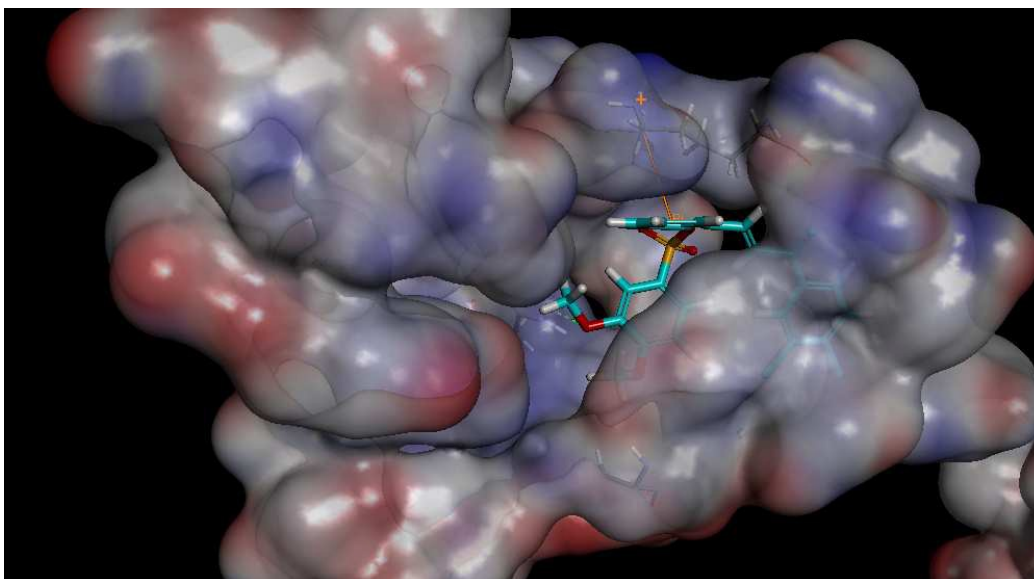


Figure 7 The docking surface model of compound **6b** with microtubule 1SA0.

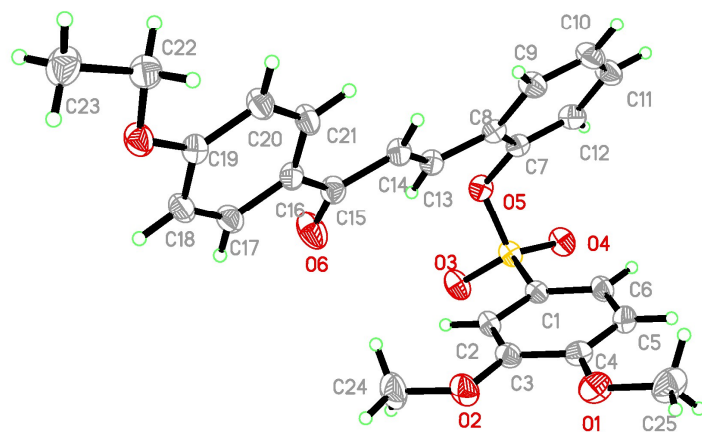


Figure 8. The crystal structure of compound **10b**

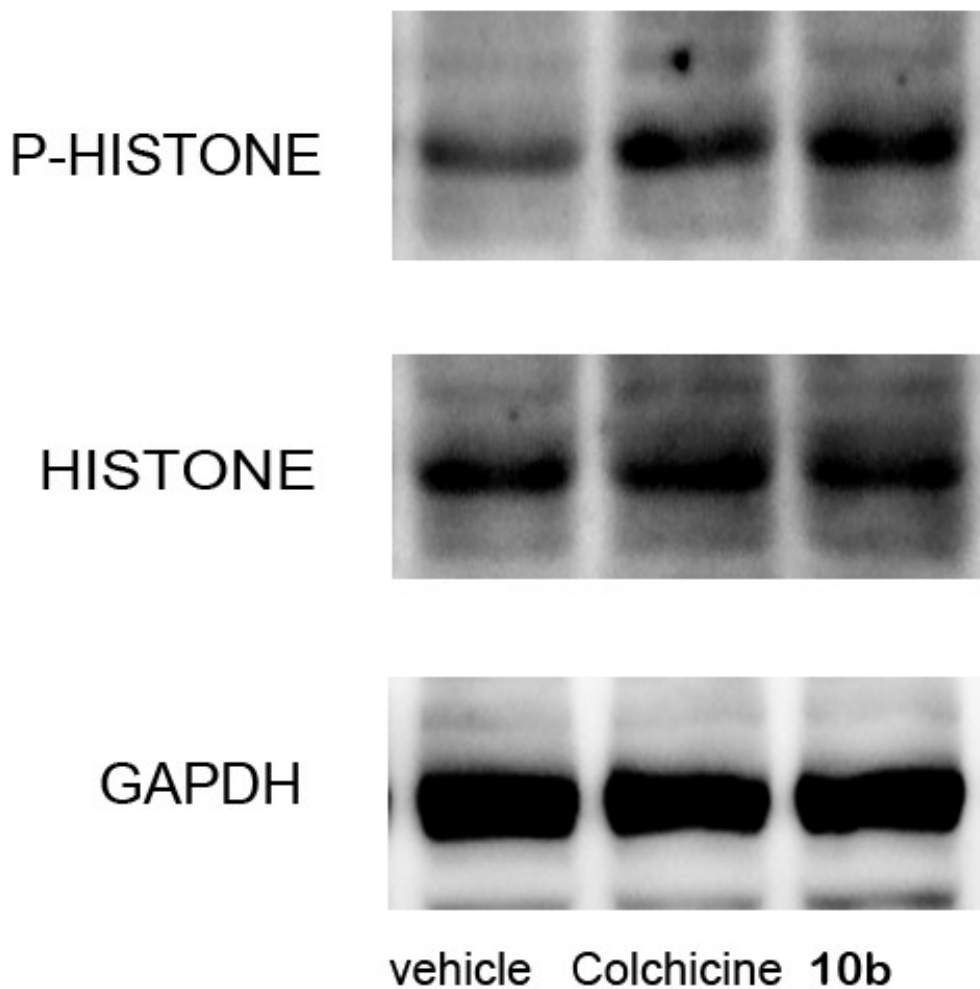
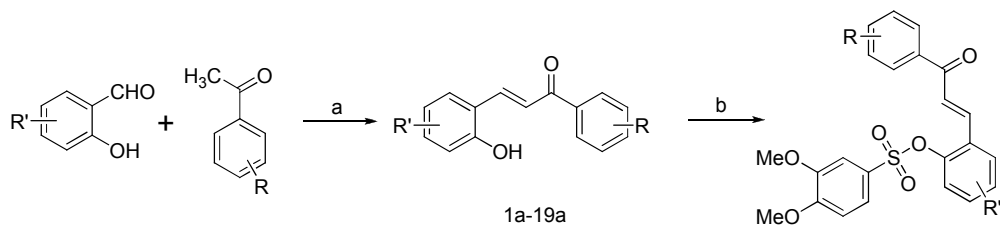


Figure 8 Treatment of 10b and colchicine caused mitotic arrest. MCF-7 cells were treated with colchicine (200 nM) and compound **10b** (200 nM). The blot was hybridized with antibodies specific for phosphorylated histone and histone. GAPDH was used as a loading control.

scheme 1<sup>a</sup> Synthesis of compounds **1b** to **19b**.



<sup>a</sup> Reagents and conditions: (a) NaOH aqueous solution (40%) in methanol, 12 hours, room temperature, 70%-90%;  
(b) Et<sub>3</sub>N in CH<sub>2</sub>Cl<sub>2</sub>, 2 hours, room temperature, 60%-75%.